Eleventh International Conference on CFD in the Minerals and Process Industries
CSIRO, Melbourne, Australia
7-9 December 2015

PRELIMINARY CFD STUDIES OF A CONTINUOUS INDUSTRIAL SCALE FLUIDIZED BED ROASTER

Swagatika DASH, Rahul K. SONI, Swati MOHANTY* and B. K. MISHRA

Process Engineering and Instrumentation, CSIR-Institute of Minerals and Materials Technology, Bhubaneswar- 751013, INDIA
*Corresponding author, E-mail address: swati.mohanty@gmail.com

ABSTRACT

Continuous fluidized bed roasters are being widely used in industries for oxidation of sulphide ores. In the present study we consider a roaster of height 24.5m, freeboard diameter of 16.85m and bed diameter of 12.5m. The distributor contains 12300 nozzles of diameter 6mm. It has two material inlets for the zinc concentrate, one gas outlet for the top product and one outlet for the bottom product. The air is blown from the bottom through four inlets for distribution across the distributor. Cooling of the bed is done by ten cooling coils inserted in the bed and water injected on the top of the bed. The feed contains around 60% particles of size ≤ 57 micron. The initial bed height is 0.8m. In this study a 3D multiphase Eulerian-Eulerian computational fluid dynamics model has been used to study the flow profile of the particles of different sizes individually (two-phase flow) as well as together (five phases). Due to the complexity of the geometry, the roaster was divided into several zones to reduce the number of cells and the computational time. Single phase simulations were carried out with 2.4 million, 3.2 million as well as 4.3 million cells and it was found that for preliminary studies a computational domain consisting of 2.4 million cells would suffice. Simulations were carried out on a HPC with 32 nodes. It was seen that there was considerable difference in the flow profiles in the case of two-phase and five-phase flow for finer particles due to resistance offered by larger size particles on the flow of finer particles.

NOMENCLATURE

C_{1s} constant
C_{2s} constant
e coefficient of restitution for particle collision
F_D drag force
g radial distribution function
G generation of turbulence kinetic energy
k turbulence kinetic energy
K momentum exchange co-efficient
p pressure
p_d solids pressure
U velocity
α volume fraction
ε turbulence dissipation rate
ρ density
η turbulent diffusivity
ν kinematic viscosity
σ Prandtl number
τ^t turbulent stress tensor
Θ granular temperature
Π influence of dispersed phase turbulence on continuous phase

Subscript
a air
d dispersed phase

INTRODUCTION

Fluidized beds have been used in chemical industries for many decades now. The first ever roaster for sulphide minerals was designed by Lurgi in 1950, which was later acquired by Outotec. However, in-depth studies involving first principle modelling of industrial scale fluidized bed are still lacking. Although sophisticated tools such as CFD have solved the problem to some extent, the hardware architecture has still not been able to handle such computationally intensive simulations. Several simplifications need to be done, to obtain approximate solutions within a reasonable time frame. Schwarz and Lee (2007) have carried out thermal CFD simulation of a fluidized bed catalytic cracking unit considering the two phases as a bubble and emulsion phase instead of a gas and particle phase to decrease the computational time for solving the transient momentum, heat and mass balance equations. An industrial scale fluidized bed polymerization reactor has been simulated by Akbari *et al.* (2013) by coupling an Eulerian-Eulerian CFD model with DQMOM population balance model, to study the flow behaviour and particle size distribution with time. Another approach for simulation of large scale gas-solid fluidized beds suggested by Lu *et al.* (2014) is using the EMMS model where the number of particles to be tracked is reduced by considering coarse grained particles, which are basically swarm of particles that temporarily move together. Schneiderbauer *et al.* (2015) have used a coarse grained two-fluid model to simulate an industrial scale polymerization fluidized bed reactor. They have used a sub-grid modification of the drag and solids stresses to account for the unresolved scales.

The major problem in simulating an industrial scale roaster is the complex geometry, size and the residence time of the particles, which range between 0.46h and 4.00h (Heukelman and Groot, 2011). In the present study an attempt has been made to simulate the flow profile of solid particles having wide particle size distribution, ranging from between 11 micron and 2373 micron, in an operational industrial scale continuous fluidized bed roaster with a complex geometry.

MODEL DESCRIPTION

Governing Equations

In the present study, Reynolds- Average Navier-Stokes (RANS) based modelling approach has been considered. The RANS equation consists of the mean and fluctuating component of the solution variables for approximating the turbulence scale. The most simple and commonly used standard k-ε turbulence model was used for the closure of the RANS equation. The phase averaged continuity equation and momentum equation for air is given by Eqns. (1) and (2), respectively (Cokljat *et al.*, 2000).

$$\frac{\partial}{\partial t}\left(\overline{\alpha_a}\rho_a\right)+\nabla\cdot\left(\overline{\alpha_a}\rho_a\tilde{U}_a\right)=0 \tag{1}$$

$$\begin{aligned}&\frac{\partial}{\partial t}\left(\overline{\alpha_a}\rho_a\tilde{U}_a\right)+\nabla\cdot\left(\overline{\alpha_a}\rho_a\tilde{U}_a\otimes\tilde{U}_a\right)\\&=-\overline{\alpha_a}\nabla\tilde{p}+\nabla\cdot\tilde{\tau}_a^t+\alpha_a\rho_a\vec{g}+F_{Da}\end{aligned} \tag{2}$$

where, $\tilde{U}_a$ is given by,

$$\tilde{U}_a=\frac{\overline{\alpha_a U_a}}{\overline{\alpha_a}} \tag{3}$$

The expression for F_{Da} is given by

$$F_{Da}=\underbrace{K_{da}\overbrace{\left(\tilde{U}_d-\tilde{U}_a\right)}^{\tilde{V}_{rel}}}_{mean-drag}+\underbrace{K_{da}\overbrace{\left(\frac{\eta_d}{\overline{\alpha_d}}\nabla\overline{\alpha_d}-\frac{\eta_a}{\overline{\alpha_a}}\nabla\overline{\alpha_a}\right)}^{-\tilde{V}_{drift}}}_{turbulent-drag} \tag{4}$$

The tilde represents the phase averaged variables while the over-bar refers to the time-averaged values. K_{da} was estimated using the Gidaspow *et al.* (1992) model.

The phase averaged momentum equation for the solid phase (*d*) is given by Eqn. (5).

$$\begin{aligned}&\frac{\partial}{\partial t}\left(\overline{\alpha}_d\rho_d\tilde{U}_d\right)+\nabla.\left(\overline{\alpha}_d\rho_d\tilde{U}_d\otimes\tilde{U}_d\right)\\&=-\overline{\alpha}_d\nabla\tilde{p}-\nabla p_d+\nabla.\tilde{\tau}_d^t+\alpha_d\rho_d\vec{g}+F_{Dd}\end{aligned} \tag{5}$$

where, p_d is given by Lun *et al* (1984) as

$$p_d=\alpha_d\rho_d\Theta_d+2\rho_d\left(1+e_{dd}\right)\alpha_d^2 g_{0,dd}\Theta_d \tag{6}$$

The solids bulk viscosity was estimated using equation presented by Lun *et. al.* (1984) and the solids kinetic viscosity was estimated using the Gidaspow *et al.* (1992) model. The expression for F_{Dd} can be defined in a similar way as F_{Da}, but with an opposite sign i.e, $F_{Dd} = -F_{Da}$. Expressions used for granular temperature as well as radial distribution function can be found in the ANSYS Fluent Theory Guide (2009).

The phase averaged transport equations for the turbulence kinetic energy and its dissipation rate are given by Eqns. (7) and (8), respectively.

$$\begin{aligned}&\frac{\partial}{\partial t}\left(\overline{\alpha}_a\rho_a\tilde{k}_a\right)+\nabla.\left(\overline{\alpha}_a\rho_a\tilde{U}_a\tilde{k}_a\right)\\&=\nabla.\left(\overline{\alpha}_a\rho_a\frac{\nu_a^t}{\sigma_k}\nabla\tilde{k}_a\right)+\overline{\alpha}_a\left(G_a-\rho_a\tilde{\varepsilon}_a\right)+\prod_{ka}\end{aligned} \tag{7}$$

$$\begin{aligned}&\frac{\partial}{\partial t}\left(\overline{\alpha}_a\rho_a\tilde{\varepsilon}_a\right)+\nabla.\left(\overline{\alpha}_a\rho_a\tilde{U}_a\tilde{\varepsilon}_a\right)\\&=\nabla.\left(\overline{\alpha}_a\rho_a\frac{\nu_a^t}{\sigma_\varepsilon}\nabla\tilde{\varepsilon}_a\right)+\overline{\alpha}_a\frac{\tilde{\varepsilon}_a}{\tilde{k}_a}\left(C_{1\varepsilon}G_a-C_{2\varepsilon}\rho_a\tilde{\varepsilon}_a\right)+\prod_{\varepsilon a}\end{aligned} \tag{8}$$

$\prod_{ka}$ is the modified form of Simonin (1990) model given as

$$\prod_{ka}=\sum_{q=1}^{M}\frac{K_{qa}}{\alpha_a\rho_a}\left(\tilde{k}_{qa}-2\tilde{k}_a+\tilde{V}_{rel}\cdot\tilde{V}_{drift}\right) \tag{9}$$

where, M is the number of secondary phases and $\tilde{k}_{qa}$ is the covariance of the velocities of continuous phase and the dispersed phase. $\prod_{\varepsilon a}$ is obtained using the model given by Elghobashi and Abou-Arab (1983). The equations used for calculation of G_a can be found in the ANSYS Fluent Theory Guide (2009).

NUMERICAL SIMULATION

Geometry Creation

A 3D geometry of the roaster was created using ANSYS Design Modeler. The height of the roaster was 24.5m, the freeboard diameter was 16.85m and the bed diameter was 12.5m. The distributor contained 12300 nozzles of diameter 6mm. There were two material inlets for the solids, one gas outlet for the top product and one outlet for the bottom product. There were four air inlets. The air inlet in the section near the feed inlet was in the vertical direction, whereas the other three were at an angle, separated by an angle of 120^0. Ten cooling coils were present in the bed section. As the geometry is quite complex, several simplifications were made. The cooling coil was represented by a single turn only, keeping the surface area the same as that of the actual coil. The distributor was considered as a porous zone with the porosity taken to be the same as the fraction of the total area of the distributor occupied by the nozzles. The geometry is shown in Figure 1.

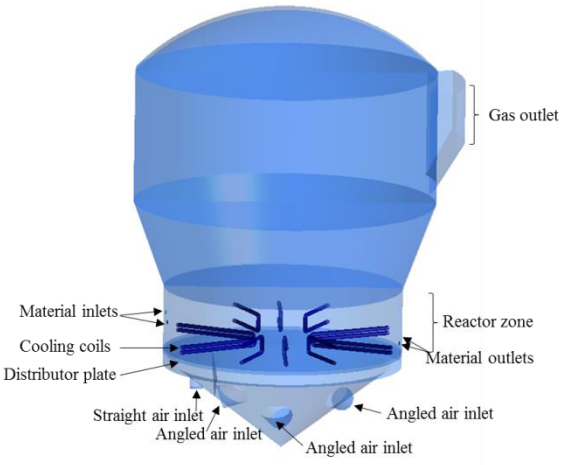

Figure 1:Simplified geometry of the fluidized bed roaster.

Meshing

The entire geometry was divided into ten zones for meshing using ANSYS Mesh Generator, since uniform size meshing in the entire geometry would lead to a very large number of computational cells and would be impossible to solve with the presently available computer

hardware. Therefore a finer mesh was used in the distributor plate, windbox and bed region with the cooling coils. Medium size mesh was used in the zone above the bed through to the gas outlet. Coarser mesh was used in the zone above the gas outlet. Meshing was tried with different sizes. Meshing in the lower part of the domain was particularly difficult due to the presence of cooling coils and four air inlets. Since the regions above the bed region are not so complex, a structured meshing was performed, whereas unstructured meshing was used in the bed and wind box region. The computational domain was divided into 2.1 million, 2.4 million, 3.2 million as well as 4.2 million cells for studying the grid independency. Unsteady state simulations with single phase were carried out for two minutes with all of the above meshes. It was found that with 2.4 million and 3.2 million cells, there was no significant difference in the velocity profile. The velocity profiles were almost identical for 3.2 million and 4.3 million cells. Therefore, considering the computational time, and the number of solid phases for multiphase simulations, it was decided to carry out the simulations with 2.4 million cells. The mesh for 2.4 million cells at y=0 is shown in Figure 2.

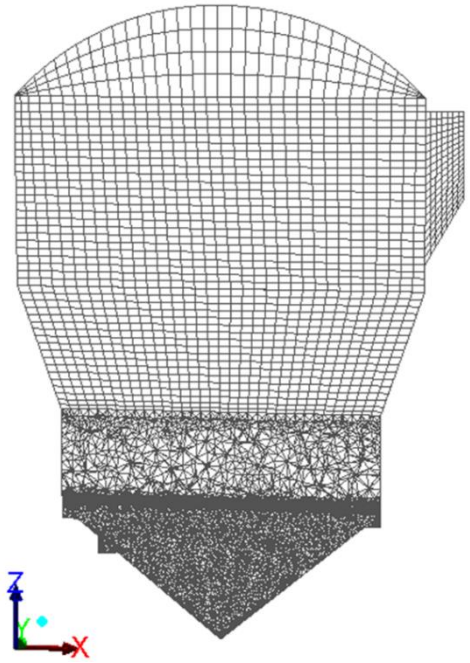

Figure 2: Mesh with 2400000 cells at y=0.

Single Phase Studies

Single phase air flow inside the domain was simulated using the 3D steady state RANS equations, in conjunction with the standard k-ε turbulence model. The total volumetric flow rate through the four inlets was taken as 70000Nm^3/hr. Isothermal condition was assumed with the temperature in the computational domain being maintained at 800^{0}C. The presence of cooling coils is only for geometry creation and no heat flow model has been incorporated in the present study. Mass flow rate for the three angled inlets was taken as 7.146kg/s, each, and for the straight vertical inlet, it was taken as one third of that of the angled air inlets (which is 2.382kg/s). The material inlets and outlets (overflow) were specified as wall, as no solids were considered. The pressure at the gas outlet was specified as -9.806 Pa (gauge). The porosity of the distributor was calculated as $2.811*10^{-3}$. Standard wall function was used at the wall for single as well as multi-phase simulations. The boundary conditions used are shown in Table 1.

Boundary	Type
Air inlets	Mass flow inlet
Outlet	Pressure outlet
Wall	No shear
Material inlet	Wall (single phase)
	Mass flow inlet (multiphase)
Material outlet	Wall (single phase)

Table 1: Boundary conditions for the simulations.

The convergence criteria for solving the momentum, k and ε equations were set to $1*10^{-7}$. Time step was set to $1*10^{-3}$ s. The under relaxation factor for the momentum and k equations was kept at $1*10^{-6}$, whereas for ε it was $1*10^{-7}$, to get a converged solution. SIMPLE algorithm was used for pressure-velocity coupling. Second order upwind scheme was used for discretization of the momentum, k and ε equations.

Multi-Phase Studies

In the present study the particle size of the feed is assumed to vary between 11 micron and 2373 micron based on the particle size distribution of top and bottom product, as the agglomeration process in the roaster has not been incorporated in the simulation studies. Thus, the roaster behaviour is not linked with the feed granulometry and chemical composition. To reduce the number of solid phases, the particles were divided into four groups and the mass weighted geometric mean of the particle sizes in each group was taken as the mean diameter of that group. The sum of the mass of the different size particles in each group was taken as the mass of that group. Table 2 shows the mean particle size and weight percent of feed in the four groups. The density of the particle was taken as 1980 kg/m^3. 3D Eulerian-Eulerian granular multi-phase model along with standard k-ε turbulence model has been used to study the flow behaviour of solids in the fluidised bed. The velocity vector of air from single phase study was patched in the case of multi-phase simulations instead of initialising with zero velocity of air, to reduce the computational time. Initially volume fraction of 0.5 for solids was patched in the computational cells, till a bed height of 0.8m. The restitution co-efficient for all solid phases is taken as 0.9.

Average particle size, micron	Wt %
16	30.15
57	28.65
280	21.20
878	20.00

Table 2: Particle size distribution for simulations

Two Phase Simulations

Two-phase simulations were carried out with air, and only one particle size at a time. Since the residence time for the solids is quite high it was not feasible to carry out unsteady state simulations till a steady state is reached. Therefore, initially a steady state simulation was carried out for approximately 100000 iterations, without any continuous feeding of the solids. The material was then fed from the two material inlets, with solids volume fraction of 0.5 and mass flow rate of $36.5*10^3$kg/hr. Again

steady state simulations were carried out for about 5000 iterations, and then unsteady state simulations were carried out for 10s or 26s. The convergence criteria for solving the momentum, k and ε equations were set to $1*10^{-4}$. The under relaxation factor for momentum equation was $1*10^{-7}$, volume fraction equation was $1*10^{-6}$, and for k and ε it was $1*10^{-7}$. Phase-Coupled SIMPLE algorithm was used for pressure-velocity coupling. Second order upwind discretization was used for momentum, k and ε equations, and QUICK for volume fraction equation. In the present study C_{1s}=1.44, C_{2s}=1.92, σ_k=1 and σ_ε=1.3 have been used. The boundary conditions used are given in Table 1.

Multi-Phase Simulations with all Solid Fractions

After carrying out two phase studies, simulations were carried out considering all the particle sizes taken together, with the solids particle size composition shown in Table 2. A total of five phases were considered i.e. four dispersed phases and one continuous phase. Simulation of five phases using the Eulerian-Eulerian model is highly computationally intensive. Initially the solids were patched in the computational cells with their respective volume fraction up to a height of 0.8m, so that the total solids volume fraction was 0.5. As in the case of two-phase studies, steady state simulation was carried out for 66000 iterations, without any solids being fed continuously. Next, solids were fed from the two material inlets with a solids volume fraction of 0.5 and mass flow rate of $36.5*10^3$kg/hr. Steady state simulations were carried out for 15000 iterations. Then unsteady state simulation was carried out for approximately 10s. The convergence criteria for solving momentum, volume fraction, k and ε equations were set to $1*10^{-4}$. The under relaxation factors for momentum, volume fraction, k and ε equations were set to $1*10^{-4}$ to get a converged solution. The discretization scheme and pressure-velocity coupling algorithm used were the same as that for two phase simulations.

RESULTS

All the simulations were carried out using ANSYS Fluent 14.0.

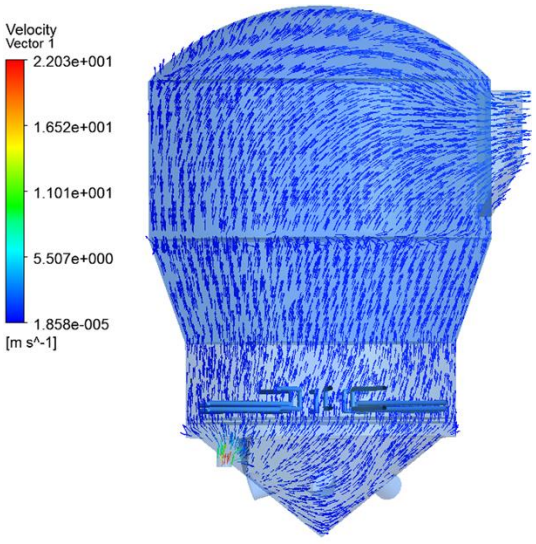

Figure 3: Single phase air velocity vector (m/s) at y=0.

Single Phase Studies

The simulated velocity vector field at y=0 for air with the inlet and boundary conditions given in the section for single phase flow is shown in Figure 3. As the cross-sectional area of the vertical air inlet was much smaller than the other three, a higher velocity was observed near it. The cooling coils did not have significant effect on the flow pattern of air.

Two Phase Studies

Figure 4(a) shows the initial condition for two phase simulation (with particle size equal to 16 micron). The vectors show the velocity of air and the contours show the volume fraction of solid particles. The profile after material is fed from the two material inlets and unsteady simulation of 26s is shown Figure 4(b). The bed has expanded considerably. Due to the flow of solids from the material inlets and its interaction with the primary phase, the air velocity vectors near the material inlets point slightly to the right.

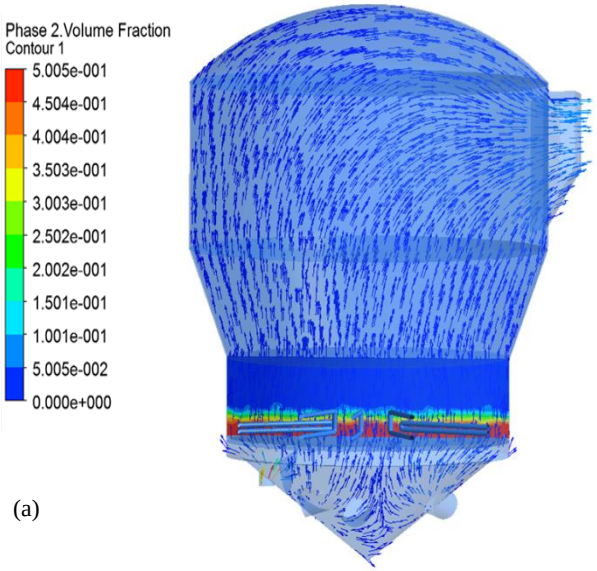

(a)

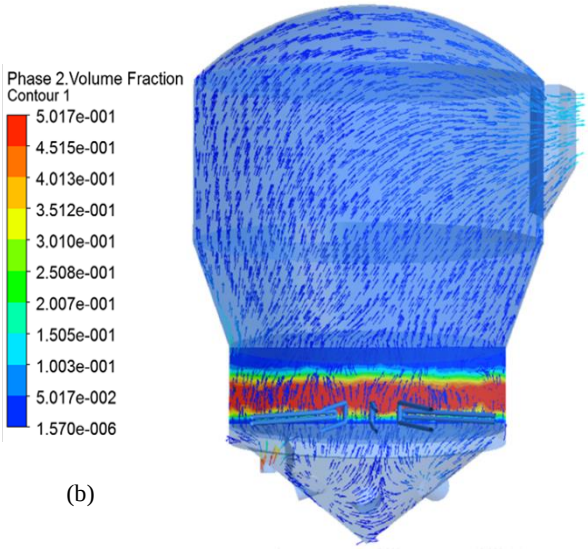

(b)

Figure 4: Volume fraction of 16 micron particles (a) with initial condition (b) after fluidization, at y=0.

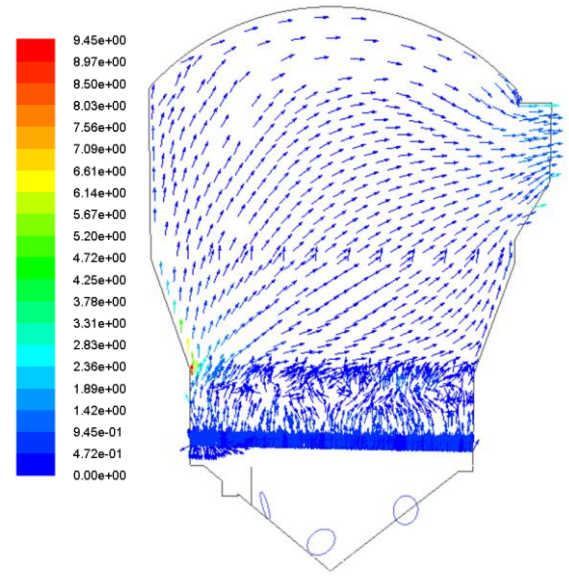

(a)

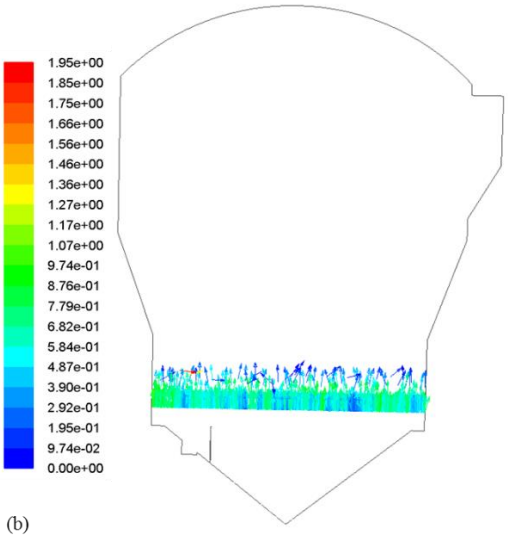

(b)

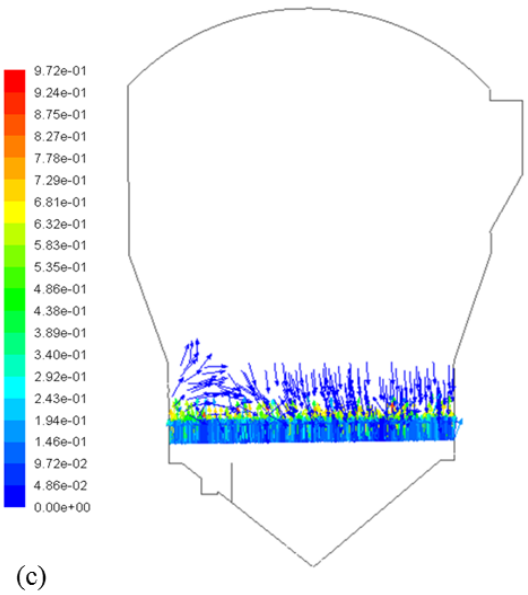

(c)

Figure 5 :Velocity vector (m/s) for two phase flow (a) 16 micron (b) 57 micron and (c) 280 micron at y=0.

Figures 5 (a)-(c) show the velocity vector of the solids for two phase simulation. Figure 5(a) shows the velocity vector for 16 micron particles. The particles move in the upward direction and some of the particles also leave the roaster from the top. The presence of cooling coils disturbs the smooth flow of the particles. Also the flow of particles from the two material inlets affects the direction of flow. Figure 5(b) shows the velocity vector for 57 micron particles. The vectors point upward, indicating that the particles have a tendency to leave the roaster from the top if sufficient time is allowed. Figure 5(c) shows the velocity vector of 280 micron particles. Near the distributor, because of higher velocity, the particles move upward, however after reaching a certain height, the gravitational force dominates over inertial force and the particles move downwards.

Multi-Phase Studies

Figures 6 (a)-(d) show the simulated velocity vector of 16, 57, 280 and 878 micron particles, respectively, when a mixture of all particle sizes are taken as feed in the fluidised bed.

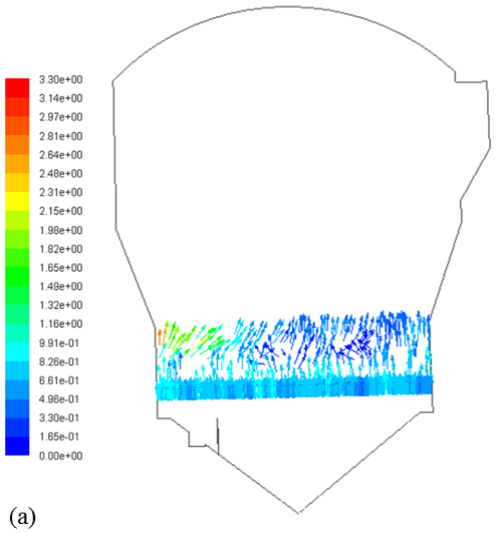

(a)

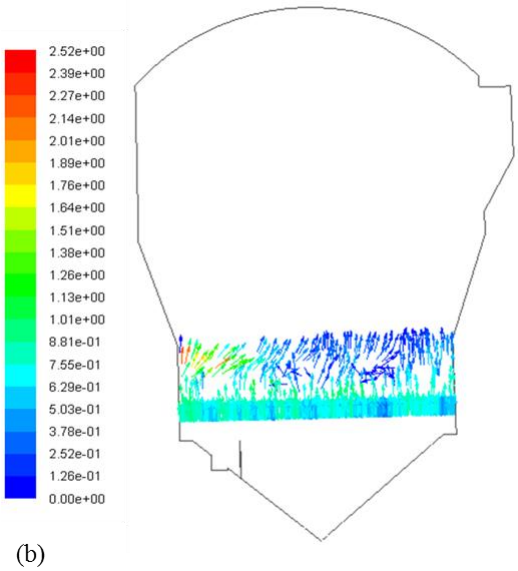

(b)

Figure 6 :Velocity vector (m/s) for multiphase flow with all size fractions (a) 16 micron (b) 57 micron at y=0.

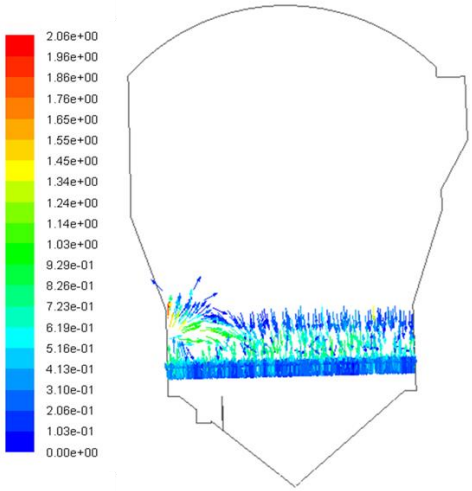

(c)

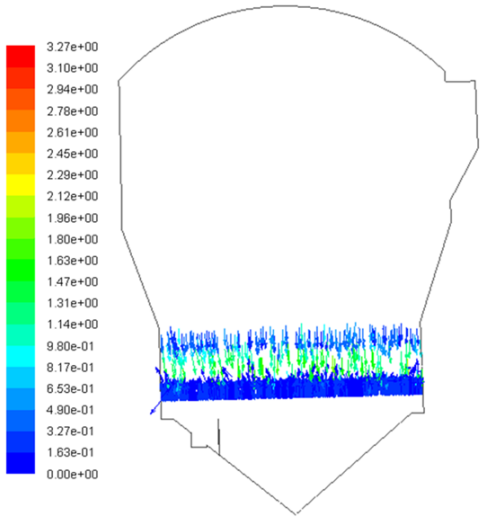

(d)

Figure 6 (cont'd.): Velocity vector (m/s) for multiphase flow with all size fractions (c) 280 micron (d)878 micron at y=0.

The presence of larger particles affects the velocity vector of finer particle as compared to the two phase simulation. It can be seen that the velocity vector of 16 micron particle (Figure 6(a)) near the material inlets is pointed more towards the right unlike in two-phase flow, where it moves in the vertical direction. The same can be noticed for 57 micron particles in Figure 6(b). This is due to the interaction between the particles. The larger particles, which are moving downward, tend to pull the finer particles also downwards. Figure 6(c) shows the velocity vector for 280 micron particles. Not much difference was observed when compared with two phase simulations. The particles tend to move downwards, except near the material inlet, where due to the high air velocity, the particles move upward up to a certain height and then circulate back to the bed. The finer particles have little effect on the larger particles. In the case of 878 micron particle (Figure 6(d)), the gravitational force is more dominant than the inertial force and therefore the particles move in downward direction.

CONCLUSION

Preliminary multi-phase Eulerian-Eulerian CFD simulation using the standard *k-ε* turbulence model have been carried out for an industrial scale continuous fluidized bed roaster. A total of five phases were considered. The simulations were computationally very intensive, particularly when all the phases were taken together. Preliminary studies show that 16 and 57 micron size particles have a tendency to leave the roaster from the top outlet, whereas 280 and 878 micron particles move up to a certain height and return to the bed. The flow of finer particles is affected by the presence of larger particles, due to particle-particle interaction. Future studies will include optimization of process parameters and use a better method to obtain solutions within a reasonable time frame.

ACKNOWLEDGEMENT

The authors acknowledge the Director, CSIR-IMMT, Bhubaneswar, India, for permission to present the paper and Hindustan Zinc Limited, Udaipur, India, for their financial support.

REFERENCES

AKBARI, V., BORHANI, T. N. G., KAZEMI, H. and HAMID, M.K.A., (2013), "Computational Fluid Dynamic and population balance modeling of industrial fluidized bed polymerization reactor", *Proc. of the 6th Int. Conf. on Process Systems Engineering*, PSE ASI, Kuala Lumpur. Malaysia, June 25-27.

ANSYS Fluent 12 Theory Guide,(2009), "Eulerian model theory", 16-41 – 16-82.

COKLJAT, D., IVANOV, V. A., SARASOLA, F. J. and VASQUES, S. A., (2000), "Multiphase k-epsilon models for unstructured meshes", *ASME 2000 Fluids Engineering Divisions Summer Meeting*, Boston, USA, June 11-15.

ELGHOBASHI, S.E., and ABOU-ARAB, T.W., (1983), "A two-equation turbulence model for two-phase flows", *Physics of Fluids*, **26**, 931-938.

GIDASPOW, D., BEZBURUAH, R. and DING, J., (1992), "Hydrodynamics of circulating fluidized beds, kinetic theory approach", *Proc. of the 7th Eng. Foundation Conf. on Fluidization*, Fluidization VII, Brisbane, Australia, May 3-8.

HEUKELMAN, S. and GROOT, D., (2011), "Fluidized bed roasting of micro-pelletized zinc concentrate: Part II–Particle entrainment and residence time", *J. of The Southern African Institute of Mining and Metallurgy*, **11**, 767-772.

LU, L., XU, J., GE, W., YUE, Y., LIU, Y. and LI, J., (2014), "EMMS-based discrete particle method (EMMS–DPM) for simulation of gas–solid flows", *Chem. Eng. Sci.* **120**, 67–87.

LUN, K.K., SAVAGE, S.B., JEFFREY, D.J. AND CHEPURNIY, N., (1984), "Kinetic theories for granular flow: inelastic particles in couette flow and slightly inelastic particles in a general flow field", *J. Fluid Mech.*, **140,** 223-256.

SCHNEIDERBAUER, S., PUTTINGER, S., PIRKER, S., AGUAYO, P. and KANELLOPOULOS, V., (2015), "CFD modeling and simulation of industrial scale olefin polymerization fluidized bed reactors", *Chem. Eng. J,*. **264**, 99–112.

SCHWARZ, M.P. and LEE, J., (2007), "Reactive CFD simulation of an FCC regenerator", *Asia-Pac. J. Chem. Eng.*, **2,** 347–354.

SIMONIN, C. and VIOLLET, P.L., (1990), "Prediction of an oxygen droplet pulverization in a compressible subsonic co-flowing hydrogen flow", In Numerical Methods for Multiphase Flows, *1990 Spring Meeting of the Fluids Engineering Division*, Toronto, Canada, June 4-7.